DOI 10.52209/2706-977X_2024_4_120 **IRSTI 55.01.85** **UDC 622.271.012.3**

The Study of the Dynamic Characteristics of the Hydro-volume Vibration Mechanism

Moyzes B.B.[1*], Kuvshinov K.A.[1], Nizhegorodov A.I.[2], Vavilova G.V.[1], Vtorushina A.N.[1]
[1]National Research Tomsk Polytechnic University, Tomsk, Russia
[2]Irkutsk National Research Technical University, Irkutsk, Russia
[*]corresponding author

Abstract. This research reviews the study of the hydro-volume vibration mechanism of Shock Vibration Source of Seismic Signals. The developed source should have a smaller weight compared to analogs due to the fact that the source is pressed to the ground at the moment of emission of the Amplitude-Modulated Sweep Signal by a falling load, Theoretical studies were carried out on a linear mathematical model of the mechanism. A comparison of the calculated values of frequency characteristics with experimental values was the method for assessing the validity of the assumptions adopted for the mathematical model. Experimental studies of the dynamic system of the mechanism were conducted on an experimental vibration stand using frequency characteristics. To simplify the design, the fall of the load for pressing is simulated by a low-frequency generator in the vibration mechanism of the experimental stand. Thus, the vibration mechanism includes two separate drives for controlling the oscillatory system for high-frequency and low-frequency oscillations, an oscillating system and an external load. The determination of frequency characteristics of the vibration mechanism, the conditions and nature of its resonance, and finding resonant zones is the task of the research.

Keywords: sweep signal, seismic vibrations, vibration mechanism, dynamic characteristics

Introduction

Various sources of seismic vibrations are used for exploration of geological environments in modern seismic exploration. At the same time, in the research works it is noted the prospects of shock-vibration sources using [1-7].

This research is a continuation of the work “The Study of the Parameters of Amplitude-Modulated Sweep Signal of the Shock Vibration Source of Seismic Signals” [1]. The overall objective of the research is to develop a small-sized seismic shock-vibration source with an amplitude-modulated probing signal.

The article reviewed [1] the probing signals with different forms of the envelope of the amplitude of the force. The prospects of using a signal with a sinusoidal envelope are confirmed. To form such a signal, it is proposed a design scheme of the seismic signal source, including an oscillatory system with an impact unit. The force and the form of the signal envelope are formed by the process of interaction of the fallen active load with the shock absorber of the actuator.

The hydro-volume vibration mechanism [8-14] can be represented as a generalized dynamic circuit, adding additional connections to it due to the presence of a resonant circuit (Fig. 1) (regardless of the materials of the elements) [15, 16].

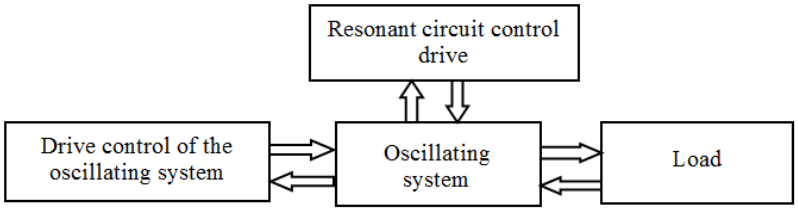

Fig 1. – Scheme of the dynamic system of the hydrovolume vibration mechanism

It is evident from the diagram of the dynamic drive system that the oscillatory system and the load acting on it represent a single system with direct and feedback connections.

The purpose of the research is to study the vibration system of the vibration mechanism that is to determine:

- its dynamic characteristics$
- the parameters of the resonant mode;
- the degree of influence of high-frequency and low-frequency generators on the amplitude of oscillations.

Also it was the task to prove:

- the validity of simulating the fall of an active load by the operation of a low-frequency generator
- the possibility of the research on the formation of an amplitude-frequency modulated signal.

In the article on the base of the experiments:

- logarithmic amplitude-frequency and phase-frequency characteristics of a dynamic system are constructed;
- logarithmic amplitude-frequency and phase-frequency characteristics of a dynamic system are constructed;

- a comparison of the calculated dynamic parameters with experimental ones is given.

1. Theoretical Part

To simplify the design of the laboratory stand (Fig. 2), in laboratory conditions, the fall of a load with mass m was replaced by its rocking-oscillatory motion [1]. It was recorded, in this case, the amplitude x of the load's movement in the vertical direction.

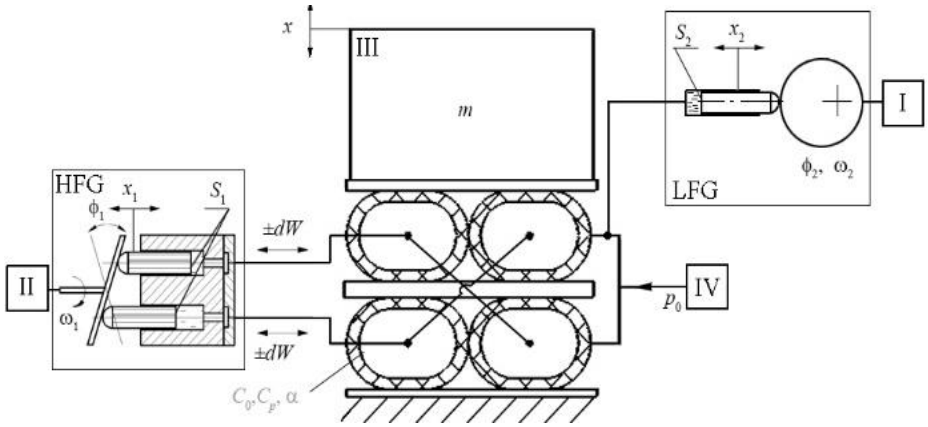

Fig 2. – Simplified schematic diagram of the experimental stand:

S_1, S_2, x_1, x_2 ω_1, ω_2 are: the area of the generators plungers and the coordinates of the plungers moving, the rotational speed of the high-frequency and low-frequency oscillation generators; φ_1 is the tilt angle of the high-frequency generator disk; φ_2 is the current position angle of the low-frequency generator shaft; p_0 is the average pressure in the system; α is coefficient of viscous losses in the vibration circuit of the mechanism; C_0 is the stiffness of the main elastic links, which includes the stiffness HPH and the stiffness due to the presence of medium pressure in the cavities; C_p is the hydraulic stiffness due to volumetric deformation; $\pm dW$ is the variable fluid flow

For this purpose, load III is placed on four cross-connected elastic shells – high-pressure hoses (HPH). The high-frequency oscillations are excited by a symmetrical generator (HFG) in them, and the shock mode is simulated by an additional low-frequency generator (LFG).

The hydrovolume vibration mechanism constructed according to this scheme consists of:

- a drive for controlling the high-frequency oscillatory system II;
- a drive for controlling the low-frequency oscillatory system I;
- an oscillating system;
- an external load III;
- medium pressure generation systems IV.

In the research [1] the general equation of displacement was obtained:

$$m\frac{d^2x}{dt^2} + \alpha \cdot \frac{dx}{dt} + C_\Sigma \cdot x = C_p \cdot k_{s1} \cdot x_1 + C_p \cdot k_{s2} \cdot x_2 \quad (1)$$

where S is the operating area of the actuator;

$k_{s1} = \frac{S_1}{S}$ and $k_{s2} = \frac{S_2}{S}$

$C_\Sigma = C_0 + C_p$.

There were obtained the equations for the system of equations for subsequent computer modeling:

$$\begin{gathered} dW = W_1 + W_2 - W_0; \\ dp = \frac{E}{W_0} dW; \\ F_d = S \cdot dp; \\ F_v = \alpha \cdot V; \\ F_x = C_0 \cdot x; \\ dF = F_d - F_V - F_x \end{gathered} \quad (2)$$

where W_1, W_2 are liquid volumes supplied by high and low frequency generators to the HPH;

W_0, dW is the initial fluid volume in the shells and its change;

E is the fluid elasticity modulus;

S is the operating area of the actuator;

dp is the pressure drop in operating cavities;

α is the coefficient of viscous losses in the oscillatory circuit;

V is the movement speed of the movable body of the actuator.

x is the current movement of the moving body;

C_0 is the stiffness of the main elastic bonds

dF, F_d, F_x, F_V are: the force transmitted through the HPH to the "ground", the driving force, the force from the current deformation of the HPH, the force of the viscous internal resistance.

A detailed structural diagram of the mechanism (Fig. 3) is given on the based on the system of equations (2).

The first adder in this structural diagram characterizes the volume balance equation and the process of forming the deformation volume *dW*, the second adder describes the force balance equation.

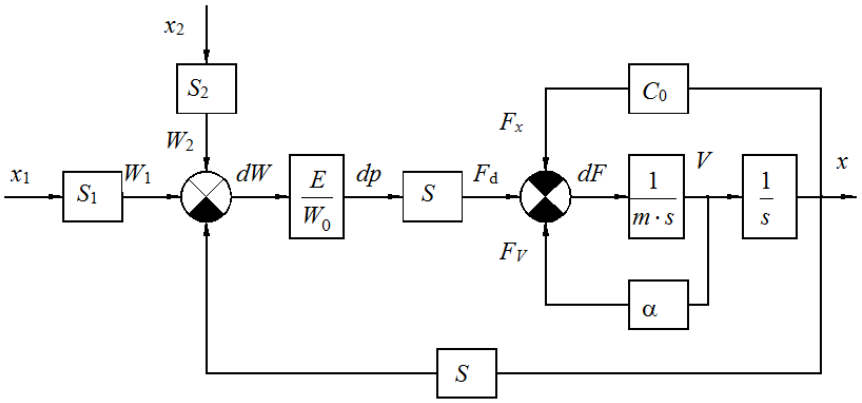

a)

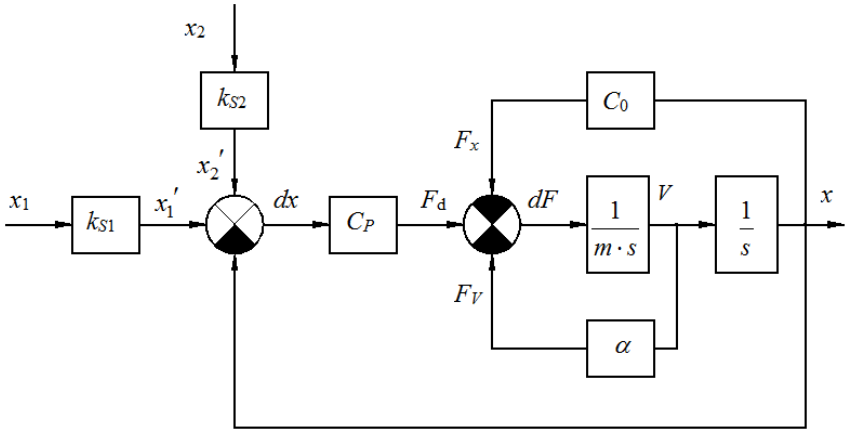

b)

Fig 2. – Structural diagrams of a hydrovolume vibration mechanism: a) for displacement, b) for pressure drop dps is the Laplace operator

According to the assumptions made when compiling the mathematical model [1], expression (1) is linear and continuous in the frequency and time interval under consideration. This allows us to perform a transformation over expression (2) - the Laplace transform:

$$(m \cdot s^2 + \alpha \cdot s + C_\Sigma) \cdot X(s) = C_p \cdot k_{s1} \cdot X_1(s) + C_p \cdot k_{s2} \cdot X_2(s) \quad (3)$$

Let's rewrite expression (3):

$$(T^2 \cdot s^2 + 2 \cdot \xi \cdot T \cdot s + 1) \cdot X(s) = k_1 \cdot X_1(s) + k_2 \cdot X_2(s), \quad (4)$$

by introducing the notations:

$$k_{1(2)} = \frac{C_p \cdot k_{s1(2)}}{C_\Sigma};$$

$$T = \sqrt{\frac{m}{C_\Sigma}} = \frac{1}{\omega_*};$$

$$\alpha = 2 \cdot \xi \cdot \sqrt{\frac{m}{C_\Sigma}}.$$

Let us consider the operation of each of the oscillation generators separately, i.e. two variants of the system operation:

- in the first case, the input is the movement of the plunger of the high-frequency generator x_1

$$(T^2s^2 + 2 \cdot \xi \cdot T \cdot s + 1) \cdot X(s) = k_1 \cdot X_1(s); \quad (5)$$

- in the second input is the movement of the plunger of the low-frequency generator x_2 :

$$(T^2s^2 + 2 \cdot \xi \cdot T \cdot s + 1) \cdot X(s) = k_2 \cdot X_2(s). \quad (6)$$

We obtain two different loading schemes for the mechanical system of the vibration mechanism, differing in:

- the nature of excitation;
- the size of the excitation volume of liquid supplied by the generators into the cavities of the shells;
- stiffness parameters.

According to the assumption of linearity [1, 17, 18] in equations (5, 6), the coefficients T, ξ and k, depending on the value of the hydraulic stiffness C_P, are constant and they are input parameters.

In a real physical model, they depend both on the generator inputs and on the change in the output parameter – the displacement x, since:

$$C_p = \frac{S(x)^2 \cdot E}{W_0}, \quad (7)$$

and therefore require correction.

We obtain the transfer functions for the system from equations (6, 7):

$$W_{x1}(s) = \frac{X(s)}{X_1(s)} = \frac{k_1}{T^2s^2 + 2 \cdot \xi \cdot T \cdot s + 1} \quad (8)$$

and

$$W_{x2}(s) = \frac{X(s)}{X_2(s)} = \frac{k_2}{T^2s^2 + 2 \cdot \xi \cdot T \cdot s + 1}. \quad (9)$$

We obtain the frequency transfer functions by applying the Fourier transform to expressions (6, 7):

$$W_{x1}(j\omega) = \frac{X(j\omega)}{X_1(j\omega)} = \frac{k_1}{1 - T^2\omega^2 + 2 \cdot j \cdot \xi \cdot T \cdot \omega} \quad (10)$$

and

$$W_{x2}(j\omega) = \frac{X(j\omega)}{X_2(j\omega)} = \frac{k_2}{1 - T^2\omega^2 + 2 \cdot j \cdot \xi \cdot T \cdot \omega}. \quad (11)$$

We determine amplitude-frequency characteristics (AFC) from the expressions (10, 11)

$$W_{x1}(\omega) = \frac{k_1}{\sqrt{(1 - T^2\omega^2)^2 + 4 \cdot \xi^2 \cdot T^2 \cdot \omega^2}} \quad (12)$$

and

$$W_{x2}(\omega) = \frac{k_2}{\sqrt{(1 - T^2\omega^2)^2 + 4 \cdot \xi^2 \cdot T^2 \cdot \omega^2}}; \quad (13)$$

- phase-frequency characteristics (PFC)

$$\varphi_{x1(2)}(\omega) = -\text{arctg}\frac{2 \cdot \xi \cdot T \cdot \omega}{1 - T^2 \cdot \omega^2} \quad (14)$$

To analyze the operation of the vibration mechanism in the future, we will use logarithmic frequency response (LFR):

$$L_{x1(2)}(\omega) = 20 \cdot \lg(W_{x1(2)}(\omega)). \quad (15)$$

By making structural transformations of the diagram (Fig. 2), we obtain for the pressure drop dp in the working cavities of the actuator:

- transfer functions:

$$W_{dp1}(s) = \frac{k_1\left(T^2s^2 + 2 \cdot \xi \cdot T \cdot s + \frac{C_0}{C_\Sigma}\right)}{T^2s^2 + 2 \cdot \xi \cdot T \cdot s + 1} \quad (16)$$

and

$$W_{dp2}(s) = \frac{k_2\left(T^2s^2 + 2\cdot\xi\cdot T\cdot s + \frac{C_0}{C_\Sigma}\right)}{T^2s^2 + 2\cdot\xi\cdot T\cdot s + 1}. \quad (17)$$

- frequency transfer functions:

$$W_{dp1}(j\omega) = \frac{k_1\left(\frac{C_0}{C_\Sigma} - T^2\omega^2 + 2\cdot j\cdot\xi\cdot T\cdot\omega\right)}{1 - T^2\omega^2 + 2\cdot j\cdot\xi\cdot T\cdot\omega} \quad (18)$$

and

$$W_{dp2}(j\omega) = \frac{k_1\left(\frac{C_0}{C_\Sigma} - T^2\omega^2 + 2\cdot j\cdot\xi\cdot T\cdot\omega\right)}{1 - T^2\omega^2 + 2\cdot j\cdot\xi\cdot T\cdot\omega}. \quad (19)$$

From expressions (18, 19) we obtain expressions for:

- AFC

$$W_{dp1}(\omega) = \frac{k_1\sqrt{\left(\frac{C_0}{C_\Sigma} - T^2\omega^2\right)^2 + 4\cdot\xi^2\cdot T^2\cdot\omega^2}}{\sqrt{(1 - T^2\omega^2)^2 + 4\cdot\xi^2\cdot T^2\cdot\omega^2}} \quad (20)$$

and

$$W_{dp2}(\omega) = \frac{k_2\sqrt{\left(\frac{C_0}{C_\Sigma} - T^2\omega^2\right)^2 + 4\cdot\xi^2\cdot T^2\cdot\omega^2}}{\sqrt{(1 - T^2\omega^2)^2 + 4\cdot\xi^2\cdot T^2\cdot\omega^2}} \quad (21)$$

- PFC

$$\varphi_{dp1(2)}(\omega) = -\text{arctg}\frac{2\cdot\xi\cdot\omega\cdot C_p}{(C_\Sigma - m\cdot\omega^2)\cdot(C_0 - m\cdot\omega^2) - 4\cdot\xi^2\cdot T^2} \quad (22)$$

To analyze the operation of the vibration mechanism in the future, we will use logarithmic frequency response (LFR)

$$L_{dp1(2)}(\omega) = 20\cdot W_{dp1(2)}(\omega). \quad (23)$$

2. Experimental Part

The experimental studies of the dynamic characteristics of the oscillating system of the mechanism were carried out on a stand (Fig. 1).

The stand consists of the following main elements:

• an actuating vibration element with an internal diameter of d_{BH} =0.01 m and an operating pressure of P_{work}=24 MPa;

• a volumetric axial-type oscillation generator with adjustment of the supplied volume $W_1=x_1\cdot S_1$by changing the stroke value x_1 of pistons with an area of $S_2=2.6\cdot10^{-4}$ m^2;

• a volumetric axial-type oscillation generator with adjustment of the supplied volume $W_2=x_2\cdot S_2$ by changing the stroke value x_2 of the piston with an area of $S_2=2.6\cdot10^{-4}$ m^2;

• a generator drive adjustable in terms of rotation speed ω_1 andω_2;

• a system for feeding leaks, maintaining and regulating the average pressure in the operating cavities of the hosepipes.

The mass of the moving parts of the mechanism is $m\approx4$ кН·sec^2/m.

The experiment was carried out with separate excitation of elastic shells by generators.

The purpose of the experiment is to determine the values of the resonance frequencies of the displacement x and the pressure drop dp.

The next values were determined in the result of the experiment:

- the resonance frequencies of the displacement of the "output link" x

  - the main ω_x:

$$\omega_x = \sqrt{\frac{C_\Sigma}{m}} \approx \text{Hz}; \quad (23)$$

  - additional $\omega_x'\approx13...18$ Hz;

- pressure drop resonance frequencies dp:

  - "positive" $\omega_{dp}=\omega_x=\omega_0$;

  - "negative"

$$\omega'_{dp} = \sqrt{\frac{C_0}{m}} \approx 3.5 \text{ Hz}. \quad (24)$$

- relative damping coefficient

$$\xi = \frac{d\omega}{\omega_0} \approx 0.1 \text{ m}^2/\text{H}. \quad (25)$$

There were determined the system parameters based on the data (23-25):

• rigidity – $C_\Sigma \approx 2.5$ MH/m, $C_p \approx 0.6$ MH/m, $C_0 \approx 1.9$ MH/m

• viscous loss coefficient $\alpha \approx 200$ Hsec/m

We obtain the calculated frequency response and phase response for displacement x and pressure drop dp for both generators (Fig. 4, 5) for different values of their amplitudes X_1 and X_2, substituting the values into expressions (12-15, 20-24).

The calculated resonance peaks coincide in frequency with the experimental ones due to the fact that the parameters determined from the experiment were substituted into the expressions. At the same time, a comparison of the nature of the asymptotes and the resonance values allows us to conclude about the admissibility of the accepted linearity.

Conclusion

The analysis of the diagrams (Fig. 4, 5) showed:

• that the slope and position of the calculated and experimental LAFC and LPFC qualitatively coincide, and the magnitude of the resonance peaks lies within the error limits of 15%;

• that the maximum LAFC for displacement x is observed in the case when the phase angle between the input $x_{1(2)}$ and the output x $\varphi_{x1(2)}$ (2) is equal to $-\pi/2$;

• the resonance in pressure drop occurs at frequencies ω_0, ω'_{dp} with a phase shift $\varphi_{dp}(2)$ equal to $+\pi/2$;

• in the transresonant mode at $\omega \to \infty$ the magnitude of the oscillation amplitude of the "output link" tends to zero, and the pressure drop remains practically unchanged.

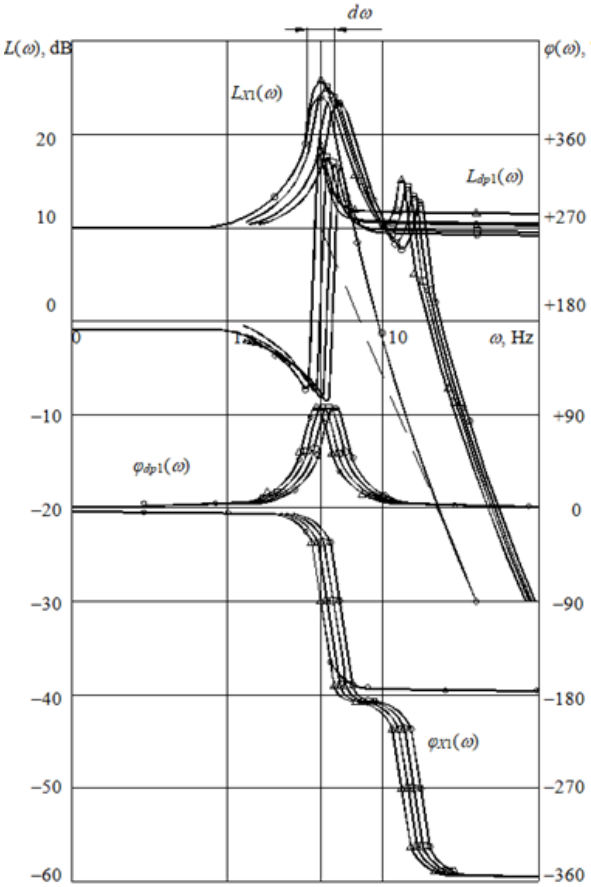

Fig. 4 – LAFC and LPFC of the high-frequency generator: o- calculated; Δ - X_1=2 mm, □ - imput X_1=1.5 mm, ⬠ - X_1=1 мм, ⎔ - imput X_1=0.5 mm

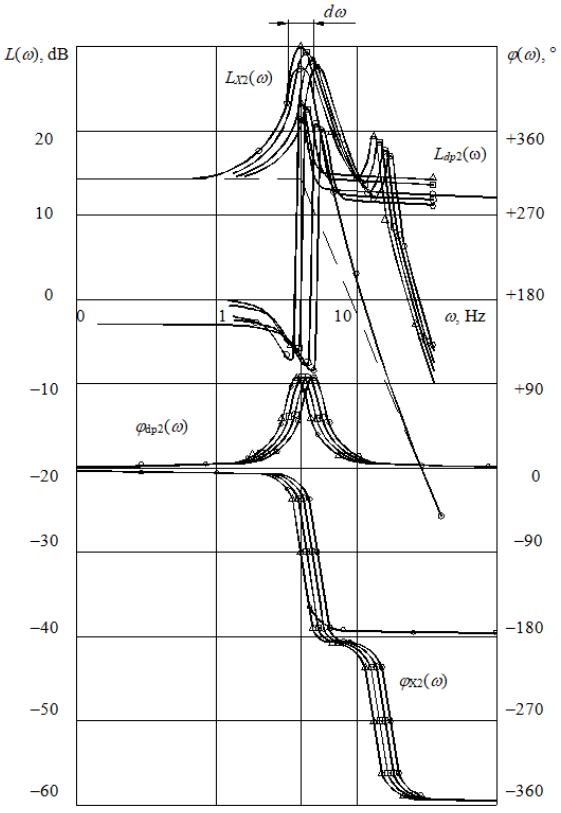

Fig. 5 LAFH and LPFC of the low-frequency generator: o- calculated; Δ - X_1=2 mm, □ - input X_1=1.5 mm, ⬠ - X_1=1 mm, ⎔ - input X_1=0.5 mm

The experimental study method of the dynamic characteristics of the mechanism in two stationary modes (first with one high-frequency generator operating, then with a low-frequency generator) consisted of obtaining experimental amplitude-frequency and phase-frequency characteristics of the following quantities:

- output signal x;
- pressure drop dp;
- phase shift angles $\varphi_{x1(2)}$ and $\varphi_{dp1(2)}$.

References

[1] Moyzes B.B., Nizhegorodov A.I. The Study of the Parameters of Amplitude-Modulated Sweep Signal of the Shock Vibration Source of Seismic Signals // Engineering Materials, 2023, Part F1222. – P. 91-128. doi: https://doi.org/10.1007/978-3-031-38964-1_7.
[2] Verstraete J.-B., Foroozandeh M. Improved design of frequency-swept pulse sequences // Journal of Magnetic Resonance, 2022, Vol. 336. – 107146. doi: 10.1016/j.jmr.2022.107146.
[3] Tang X., Suddarth S., Kantesaria S., Garwood M.: A frequency-swept, longitudinal detection EPR system for measuring short electron spin relaxation times at ultra-low fields // Journal of Magnetic Resonance, 2022, Vol. 342. – 107279. doi: https://doi.org/10.1016/j.jmr.2022.107279
[4] Wang L., Li H.: GBO algorithm for seismic source parameters inversion // Geodesy and Geodynamics, 2022, Available online. – P.1-2. doi: https://doi.org/10.1016/j.geog.2022.06.004.
[5] Poletto F., Schleifer A., Zgauc F., Meneghini F., Petronio L.: Acquisition and deconvolution of seismic signals by different methods to perform direct ground-force measurements // Journal of Applied Geophysics, 2016, Vol. 135. – P. 191-203 (2016).
[6] Alifov A.A. On the calculation by the method of direct linearization of mixed oscillations in a system with limited power-supply // Advances in Computer Science for Engineering and Education II, 2020. – P. 23-31. doi: https://doi.org/10. 1007/978-3-030-16621-2_3
[7] Brenes A., Juillard J., Ayala J. et al. Experimental validation of a novel characterization procedure based on fast sweep measurements for linear resonators with a large time constant // Mechanical Systems and Signal Processing, 2025, Vol. 225. – 112252.
[8] Alifov, A.A. Oscillations for delayed elastic constraint and a limited power energy source// J. Mach. Manuf. Reliabil, 2020. – Vol. 49(2). – P. 105–109.
[9] Ahirrao N.S., Bhosle S.P., Nehete D.V. Dynamics and Vibration Measurements in Engines // Procedia Manufacturing, 2018, vol. 20, pp. 434–439.
[10] Halit E. Acceleration, Vibration, and Shock Measurement. Abingdon, Taylor & Francis Group, CRC Press LLC. 2000. – 950 p.
[11] Nizhegorodov A.I., Gavrilin A.N., Moyzes B.B., Kuvshinov K.A. Hydraulic drive of vibration stand for testing the robotic systems units by random vibration method // IOP Conference Series: Materials Science and Engineering, 2019, Vol. 516(1). – 012031. doi: 10.1088/1757-899X/516/1/012031
[12] Plotnikova I., Vedyashkin M., Mustafina R., Plotnikov I., Tchaikovskaya O., Bastida J., Verpeta M. Optimization of the Stabilization System for Electromagnetic Suspension in Active Vibration Isolation Devices // MATEC Web of Conferences, 2016, Vol. 79. – 01019. https://doi.org/10.1051/matecconf/20167901019.
[13] Nizhegorodov A I, Gavrilin A N, Moyzes B B, Cherkasov A I, Zharkevich O M, Zhetessova G S, Savelyeva N A. Radial-piston pump for drive of test machines // IOP Conf. Series: Materials Science and Engineering, 2018, Vol. 289 (1). – 012014. doi:10.1088/1757-899X/289/1/012014
[14] Sikhimbaev M.R., Sherov K.T., Zharkevich O.M., Sherov A.K., Tkachyova Y.O. Experimental studies of stabilization of boring cutter form - building top oscillation // Journal of Vibroengineering, 2012, Vol. 14, no 2. – P. 661-670
[15] Surzhikov A.P., Lysenko E.N., Malyshev A.V., Vlasov V.A., Suslyaev V. I., Zhuravlev V.A., Korovin E.Y., Dotsenko O.A. Study of the Radio-Wave Absorbing Properties of a Lithium-Zinc Ferrite Based Composite // Russian Physics Journal, 2014, Vol. 57(5), P. 621-626 (2014). doi: 10.1007/s11182-014-0284-9.
[16] Lysenko E.N., Surzhikov A.P., Vlasov V.A., Malyshev A.V., Nikolaev E.V. Thermal analysis study of solid-phase synthesis of zinc- and titanium-substituted lithium ferrites from mechanically activated reagents // Journal of Thermal Analysis and Calorimetry, 2015, Vol. 122. – P. 1347-1353. doi: 10.1007/s10973-015-4849-9.
[17] Moyzes B., Gavrilin A., Kuvshinov K., Smyshlyaev A., Koksharova I. Using the Vibration Recorder Mobile Diagnostic Complex for Studying Vibration Processes //Material and Mechanical Engineering Technology, 2022, Vol. 3. – P. 50 – 57. doi: 10.52209/2706-977X_2022_3_50.
[18] Gavrilin A., Moyzes B., Cherkasov A., Mel′nov K., Zhang X. 2016 Mobile Complex for Rapid Diagnosis of the Technological System Elements //MATEC Web of Conferences, 2016, Vol. 79. – 01078 doi: 10.1051/matecconf/20167901078

Information of the authors

Moyzes Boris Borisovich, c.t.s., associate professor, National Research Tomsk Polytechnic University
e-mail: mbb@tpu.ru

Kuvshinov Kirill Aleksandrovich, senior lector National Research Tomsk Polytechnic University
e-mail: kuvshinov@tpu.ru

Nizhegorodov Anatolij Ivanovich, d.t.s, professor, Irkutsk National Research Technical University
e-mail: nastromo_irkutsk@mail.ru

Vavilova Galina Vasilevna, c.t.s., associate professor, National Research Tomsk Polytechnic University
e-mail: wgw@tpu.ru

Vtorushina Anna Nikolaevna, c.c.s., associate professor, National Research Tomsk Polytechnic University
e-mail: anl@tpu.ru